Mechanism and Machine Theory xxx (xxxx) xxx

Contents lists available at ScienceDirect

Mechanism and Machine Theory

journal homepage: www.elsevier.com/locate/mechmachtheory

Parametric design and multi-objective optimization of a general 6-PUS parallel manipulator

S. Nader Nabavi[a,b], Morteza Shariatee[a], Javad Enferadi[c], Alireza Akbarzadeh[a,*]

[a] Mechanical Engineering Department, Center of Excellence on Soft Computing and Intelligent Information Processing, (SCIIP), Ferdowsi University of Mashhad, Mashhad, Iran
[b] Department of Mechanical Engineering, University of Bojnord, Bojnord, Iran
[c] Mechanical Engineering Department, Mashhad Branch, Islamic Azad University, Mashhad, Iran

ARTICLE INFO

Article history:
Received 14 September 2019
Revised 13 March 2020
Accepted 5 April 2020
Available online xxx

Keywords:
Stewart robot
6-PUS robot
Architecture synthesis
Performance indices
Multi-objective optimization

ABSTRACT

Parallel robots usage as motion simulators is increasing. Among them, the Stewart robot is most commonly used. However, a properly selected 6-PUS architecture seems to potentially offer certain advantages over the popular 6-UPS structure. To prove this hypothesis, the FUM-Stewart-M450 robot is selected as a case study in this study. The parameters representing overall robot size and desired workspace are considered to be the same in both the 6-UPS and 6-PUS robots for a fair comparison. To fully define the 6-PUS robot, three performance indices, dexterity, kinetic energy and a new modified workspace index are used for optimal determination of the remaining parameters. The proposed workspace index is specifically designed for motion simulators. It not only considers the robot workspace in all 6 degrees-of-freedom but also takes into account the main feature of motion simulators motion cues, their return to home for each subsequent motion. The Pareto front is used to compare various 6-PUS designs with the FUM-Stewart-M450. The results indicate that among the optimized robots, there exists an architecture that significantly lowers maximum actuator's static and dynamic forces. This paper offers a general outline for optimization and comparison of various robot structures having combined rotational-translational motion.

1. Introduction

The use of robotic manipulators in industry is significantly increasing. According to the application, a robot is used either as a path generator or as a motion generator. Generally, serial configurations are more suitable for path generation applications such as machining [2] and pick and place tasks [3], since they benefit from relatively larger workspace in comparison with their counterparts. Due to the high load carrying capacity and stiffness, parallel chains are mostly used for motion generation tasks such as driving simulator [4], universal test devices [5] and in some medical applications [6]. Despite their small workspace, the use of parallel kinematic machines (PKMs) for accurate machining tasks is increasing [7–10]. Likewise, specific surgery robots have been developed [11].

The Stewart robot has received more attention among 6-DoF parallel robots. Because of that, in most literature it is used as case study. For a single robot structure there are various different architectures possible, each of which have their own

* Corresponding author.
E-mail address: ali_akbarzadeh@um.ac.ir (A. Akbarzadeh).

https://doi.org/10.1016/j.mechmachtheory.2020.103913
0094-114X/

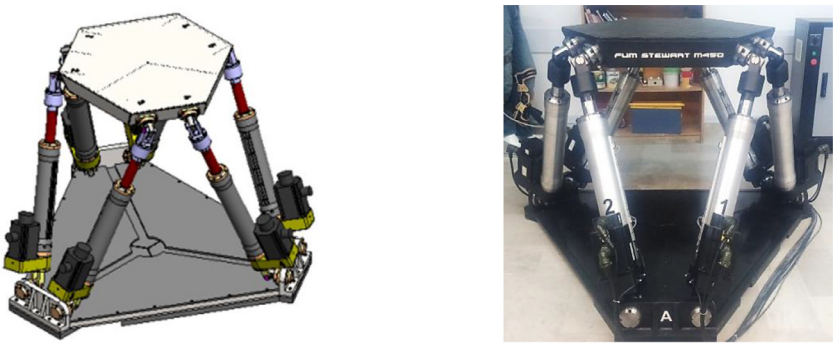

Fig. 1. FUM-Stewart M450 robot, a) Cad Model, b) Robot prototype.

pros and cons. Ma and Angeles [12] investigated parallel robots architecture from the design point of view and the need to use optimization in order to avoid singular architectures. Moreover, nowadays there are more important criteria for robot optimization than singularity alone. Different performance indices were introduced to optimize parallel robots. Workspace index [13,14] is one of the most important kinematic indices, although it is not solely sufficient for kinematic and dynamic evaluation of a robot. As a result, indices such as manipulability concept [15], dexterity [16,17] and stiffness [18] have also been introduced.

The lack of study on other 6-DoF parallel structures has attracted the attention of many researchers toward 6-PUS mechanism as an alternative to the well-known Stewart robot. One of the early robots with 6-PUS structure is the INRIA active wrist [19]. Specific 6-PUS robot architectures such as HexaM, HexaGlide and Hexaslides [20,21] have been introduced, since there can be different architectures by proper positioning of joints and selection of geometric parameters. Kinematics and dynamics of a general parametric 6-PUS robot have been studied well [22]. In addition, to meeting a predefined workspace, architecture and dimensional optimization of such a robot was carried out, using penalty function in the optimization algorithm [23]. Condition number and minimum singular value were used for optimization of geometrical parameters of an asymmetric Stewart platform to obtain dexterous workspace [24]. Khan et al. [25] have proposed a new scaling factor for Jacobian matrix normalization. Also, a multi-objective optimization was performed on 6-PUS robot with inclusion of workspace, isotropy, kinematic sensitivity and inertial characteristics indices.

Parallel robots with 6-DoF have a combined rotational and translational workspace which leads to an inhomogeneous Jacobian matrix. Consequently, the results of ordinary kinematic indices are not reliable. To overcome this issue several methods [26,27] have been presented to homogenize the Jacobian matrix, while choice of normalization methods and parameters are arbitrary. On the contrary, a new recently developed index, called kinetic energy index, KEI [1] presents a unique solution for Jacobian homogenization. The definition of KEI is based on the transferred kinetic energy from robot actuators to the payload causing it to be invariant from the dimension of Jacobian arrays.

Recently, Thales has claimed that their brand-new motion simulator with 6-PUS structure is more efficient than the conventional models with Stewart structure in terms of power consumption, in spite of the fact that to the best of our knowledge there is no theoretical proof available yet. Thus, this research study aims to find an optimum architecture of the 6-PUS robot as an alternative for a readily available Stewart motion simulator while considering new performance indices. The Stewart robot used for comparison of the results is a general motion simulator constructed in the Robotics laboratory of the Ferdowsi University of Mashhad, called FUM Stewart M450. The optimum robots are obtained by simultaneously making use of three performance indices including workspace, dexterity and kinetic energy using genetic algorithm. Additionally, finding appropriate solution is restricted by dimensional constraints, obtained from the FUM Stewart M450 robot, as well as meeting desired workspace requirements. Finally, for comparison of the results, three solutions are selected from the Pareto front which inherit the maximum of each index. The results proved that there exists a specific architecture of 6-PUS robot that is better than the FUM Stewart M450 in terms of kinematic and dynamic performance.

2. Description of the FUM Stewart robot

The FUM Stewart M450 robot is depicted in Fig. 1. This parallel robot with UPS structure is comprised of six legs with active prismatic joint benefiting from six independent degrees of freedom. The term UPS stands for joints type, i.e. universal, prismatic and spherical. The robot is designed to support a payload of $M_P = 400$ kg and moment of inertia equal to $\bar{I}_P = \text{diag}(100,\ 100,\ 100)\ \text{kg.m}^2$.

In the design of the FUM Stewart M450 robot, five geometric parameters are considered including, radius of base platform, r_b, half the distance between adjacent universal joints, d_b, radius of moving platform, r_p, half the distance between adjacent spherical joints, d_p and height of the robot in home position, Z_h. The parameters are illustrated in Fig. 2.

Please cite this article as: S.N. Nabavi, M. Shariatee and J. Enferadi et al., Parametric design and multi-objective optimization of a general 6-PUS parallel manipulator, Mechanism and Machine Theory, https://doi.org/10.1016/j.mechmachtheory.2020.103913

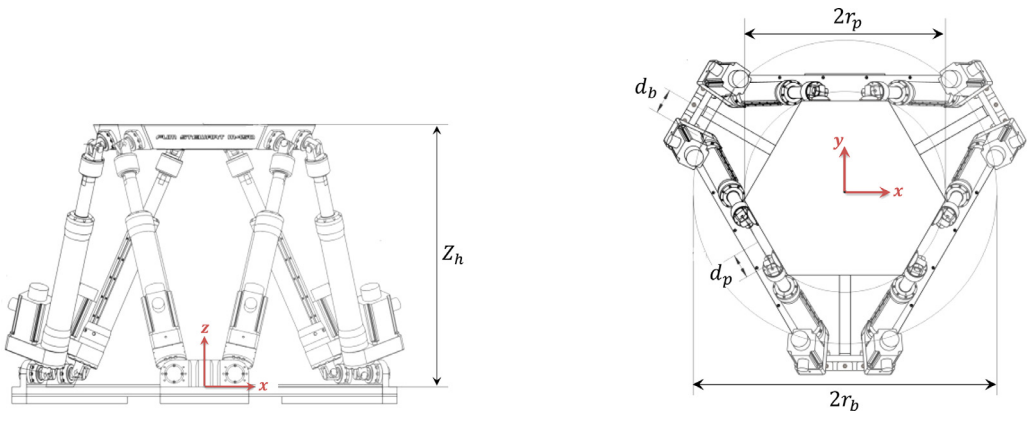

Fig. 2. Design parameters of the FUM Stewart M450

Table 1
The desired and actual workspace of the FUM Stewart M450.

Workspace	Translational movement						Rotational movement					
	Surge (cm)		Sway (cm)		Heave (cm)		Roll (deg)		Pitch (deg)		Yaw (deg)	
Desired	± 25		± 25		± 12		± 14		± 14		± 20	
Actual	−38	+38	−41	+41	−13	+21	−25	+17	−19	+19	−48	+48

Table 2
Dynamic parameters of the FUM Stewart M450 robot.

Components of the robot	Description	Parameter	Value
Link	Total mass	$\boldsymbol{M_l}$	55 **kg**
	Stroke length	$\boldsymbol{S_t}$	0.30 **m**
Moving platform	Mass	$\boldsymbol{m_p}$	50 **kg**
Payload	Mass	$\boldsymbol{M_p}$	400 **kg**
	Moment of inertia	${}^{T}\bar{\mathbf{I}}_p$	$\begin{bmatrix} 100 & 0 & 0 \\ 0 & 100 & 0 \\ 0 & 0 & 100 \end{bmatrix}$ **kg.m**^{2}

The optimal robot is designed and constructed using design parameters according to workspace requirements. The desired workspace consists of constant constraints defined for robot movement in opposing directions for each degree of freedom. The selected robot must have a workspace equal to or greater than the desired workspace, also known as actual workspace. In other words, the desired workspace is a subset of the actual workspace. Table 1 shows the values of the desired and actual workspaces of the optimum FUM Stewart M450 parallel manipulator.

The design parameters of the robot have been optimized so that the static and dynamic forces of the actuators are minimized. In the static analysis, the position and orientation of the robot are simultaneously considered, whereas for dynamic analysis, six specific trajectories for each degree of freedom are used. Given the dynamic parameters as shown in Table 2, the maximum values of the static and dynamic forces of the robot were calculated as 4.7 KN and 6.9 KN, respectively.

3. The description of 6-PUS robot

3.1. Geometry

The 6-PUS robot consisting of six kinematic chains, resembles the 6-UPS robot with the same joint types. Likewise, the active joint in the 6-PUS robot is also prismatic. The advantages of the 6-PUS robot can be pointed out as reduction of the risk of collision of the moving parts as well as higher load capacity. Fig. 3 shows the geometric design parameters of the 6-PUS robot, which has five parameters exactly the same with 6-UPS robot. These parameters include r_b, d_b, r_p, d_p and Z_h. Two angular parameters β and γ, are considered for defining robot rails alignment and p_0 is the initial position of the robot sliders at Z_h.

As it is shown by the examples in Fig. 4, the appropriate selection of two angular parameters, β and γ, results in different 6-PUS robot architectures with unique rails arrangement. In Fig. 4a there is a vertical configuration of the 6-PUS robot for which β and γ are 150°and90°, respectively. Pure vertical motion is a feature of this type of robot. In Fig. 4b all motion sliders of the robot are located on the hexagon sides, the base platform of the FUM Stewart M450. In this type of

Please cite this article as: S.N. Nabavi, M. Shariatee and J. Enferadi et al., Parametric design and multi-objective optimization of a general 6-PUS parallel manipulator, Mechanism and Machine Theory, https://doi.org/10.1016/j.mechmachtheory.2020.103913

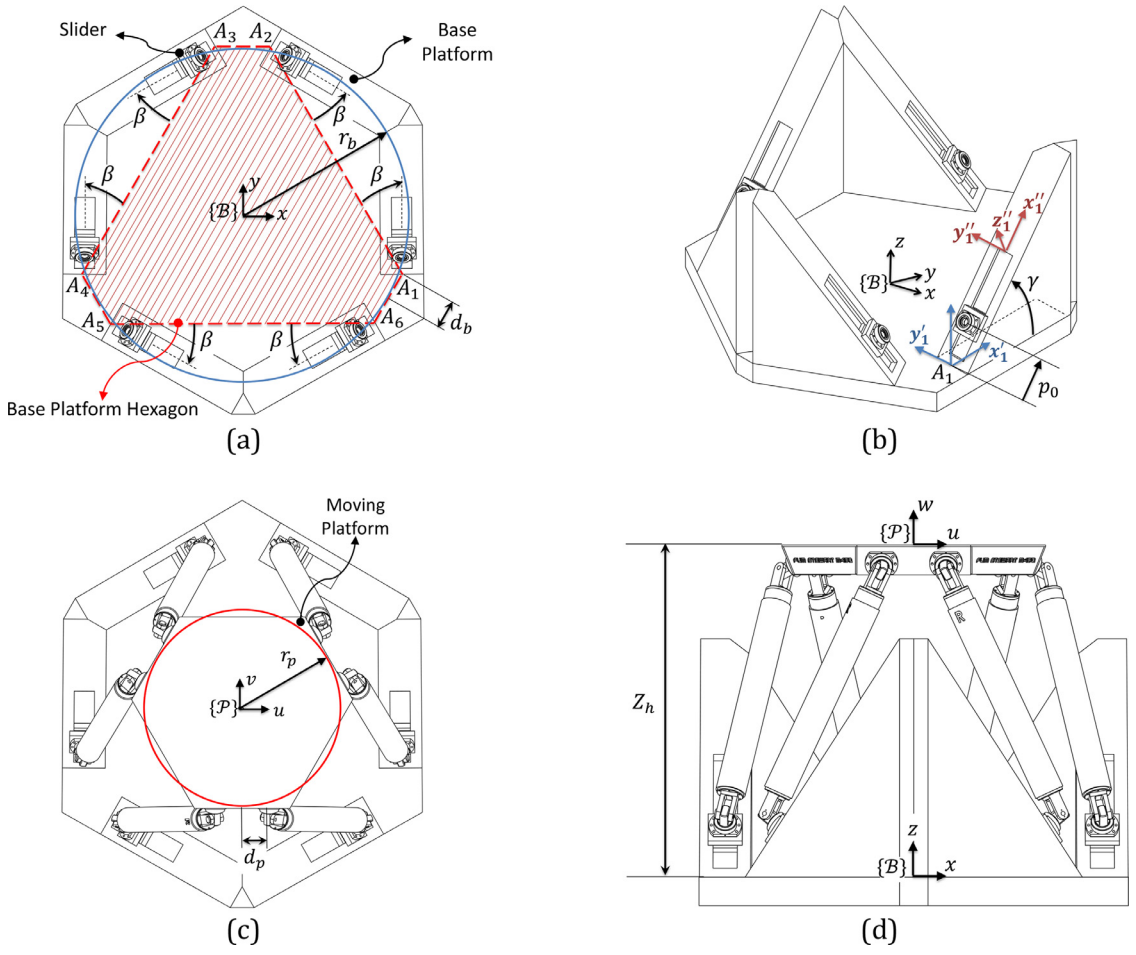

Fig. 3. The design parameters of the 6-PUS robot, a) Top view of the base platform, b) Isometric view of the base platform, c) Top view of the 6-PUS robot, d) Front view of the 6-PUS robot

configuration, the parameters β and γ are zero. By independent assignment of β for each kinematic chain, a configuration similar to that of Fig. 4c can be achieved. In this architecture pure translational movement is created along the robot rails. Fig. 4d is another configuration in which the rails are leaning outside.

The purpose of this paper is to find a suitable configuration of the 6-PUS robot that has a better performance than the current FUM Stewart M450 robot. Kinematics and dynamics analysis of general architecture 6-PUS are the prerequisites for finding the optimal robot.

3.2. Kinematics and Jacobian of the 6-PUS robot

In order to compare the workspace of the 6-PUS robot with that of the FUM Stewart M450, inverse kinematics equations are necessary. The inverse kinematics determines sliders distance from the hexagon corner for a given position of the end-effector, EE. If the distance is within the allowed range, the position of the EE can be considered as the robot's workspace. To start with inverse kinematics, the position vectors for the i^{th} kinematic chain are illustrated in Fig. 5.

The position vector of sliders, $\vec{p}_i$, can be found using the EE position vector. Eq. (1) shows the relationship between the position vectors for the i^{th} kinematic chain of the 6-PUS robot.

$$\vec{\mathbf{c}} = \vec{\mathbf{a}}_i + p_i\vec{\mathbf{e}}_i + \boldsymbol{l_u}\vec{\mathbf{m}}_i + \boldsymbol{l}\vec{\mathbf{n}}_i - \mathcal{R}\vec{\mathbf{s}}'_i \tag{1}$$

In this equation, $\vec{\mathbf{a}}_i$ is the position vector of A_i points, $\vec{\boldsymbol{e}}_i$ is the unit vector along rails, $l_u\vec{\mathbf{m}}_i$ is a constant vector perpendicular to the robot rails, l is the length of link, $\vec{\mathbf{n}}_i$ is the unit vector along the i^{th} link, $\mathcal{R}$ is the rotation matrix between the moving coordinate and the base coordinate connected to the moving platform and the base platform, respectively and $\vec{\mathbf{s}}'_i$ is the position vector of spherical joints defined in the moving coordinate. By solving the inverse kinematic equation, the position of each slider will be obtained as follows:

$$p_i = \vec{\boldsymbol{e}}_i \cdot \vec{\boldsymbol{\eta}}_i \pm \sqrt{\boldsymbol{\Delta}}, \qquad \boldsymbol{\Delta} = (\vec{\boldsymbol{e}}_i \cdot \vec{\boldsymbol{\eta}}_i)^2 - \left(\vec{\boldsymbol{\eta}}_i \cdot \vec{\boldsymbol{\eta}}_i - l^2\right) \tag{2}$$

Please cite this article as: S.N. Nabavi, M. Shariatee and J. Enferadi et al., Parametric design and multi-objective optimization of a general 6-PUS parallel manipulator, Mechanism and Machine Theory, https://doi.org/10.1016/j.mechmachtheory.2020.103913

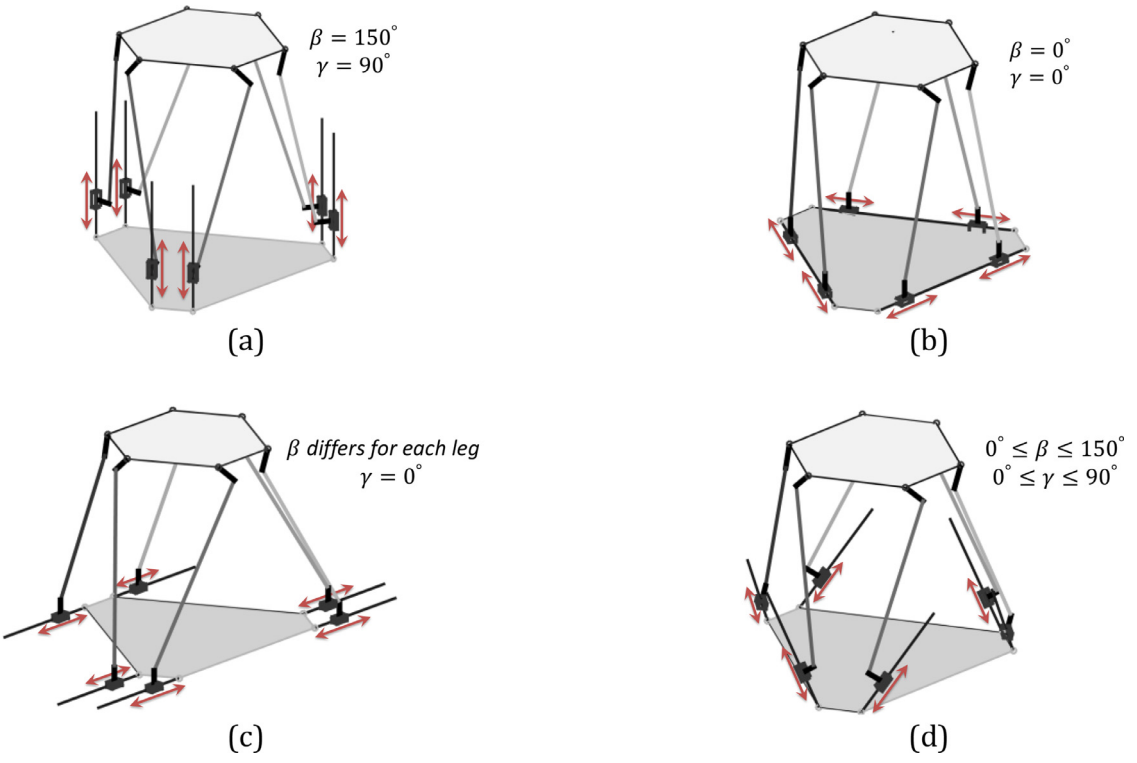

Fig. 4. Different architectures of the 6-PUS robot with a) vertical rails, b) triangular rails, c) horizontal parallel rails and d) inclined rails.

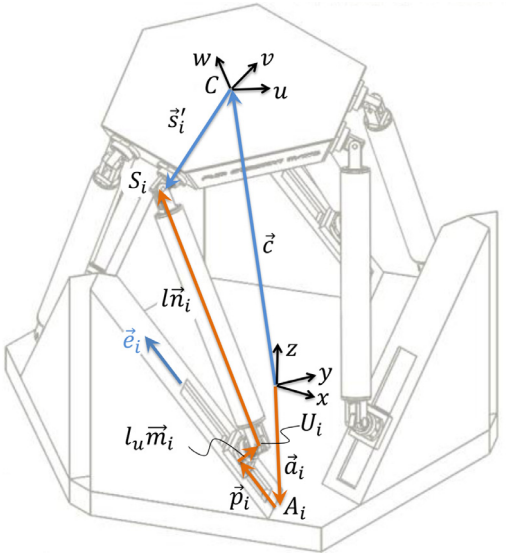

Fig. 5. The position vectors of the 6-PUS robot for the i^{th} kinematic chain

where the vector $\vec{\boldsymbol{\eta}}_i$ includes all known parameters of Eq. (1) and is defined as follows:

$$\vec{\boldsymbol{\eta}}_i = \vec{\mathbf{c}} + \mathcal{R}\vec{\mathbf{s}}_i' - \vec{\mathbf{a}}_i - l_u\vec{\mathbf{m}}_i \tag{3}$$

By using the time derivation of Eq. (1), the relationship between the velocity of EE and actuators is obtained. Defining the velocity vector of the joint space as $\dot{\mathbf{q}} = [\dot{p}_1 \quad \dots \quad \dot{p}_6]^T$ and the Cartesian velocity vector for EE as $\dot{\mathcal{X}} = [\dot{X}_C \quad \dot{Y}_C \quad \dot{Z}_C \quad \Omega_x \quad \Omega_y \quad \Omega_z]^T$, the Jacobian matrix of the general 6-PUS robot can be calculated as follows:

$$\dot{\mathbf{q}} = \mathbf{J}\dot{\mathcal{X}};\ \mathbf{J} = \mathbf{J}_{inv}^{-1}\mathbf{J}_{dir} \tag{4}$$

Please cite this article as: S.N. Nabavi, M. Shariatee and J. Enferadi et al., Parametric design and multi-objective optimization of a general 6-PUS parallel manipulator, Mechanism and Machine Theory, https://doi.org/10.1016/j.mechmachtheory.2020.103913

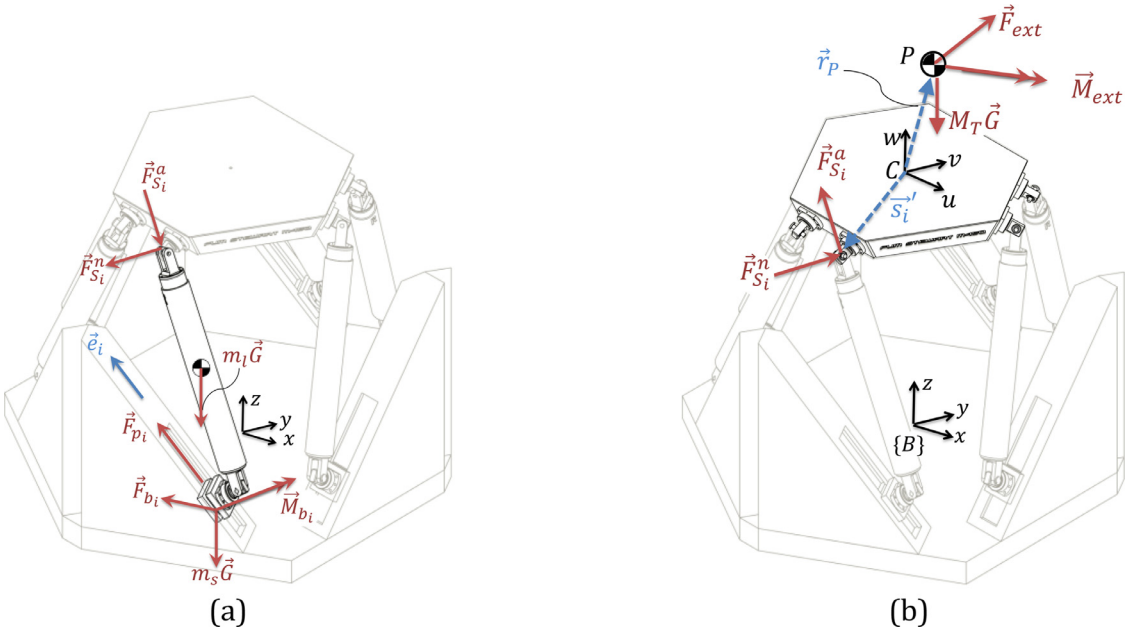

Fig. 6. The free body diagram of the a) i^{th} leg and b) moving platform of the 6-PUS robot

where $\mathbf{J}_{dir}$ and $\mathbf{J}_{inv}$ are the direct and inverse of the Jacobian matrix, respectively.

$$\mathbf{J}_{dir} = \begin{bmatrix} \vec{\mathbf{n}}_1^T & \left(\mathcal{R}\vec{\boldsymbol{s}}_1' \times \vec{\mathbf{n}}_1\right)^T \\ \vdots & \\ \vec{\mathbf{n}}_6^T & \left(\mathcal{R}\vec{\boldsymbol{s}}_6' \times \vec{\mathbf{n}}_6\right)^T \end{bmatrix}_{6\times 6} \tag{5}$$

$$\mathbf{J}_{inv} = [\mathrm{diag}((\vec{\mathbf{e}}_1.\vec{\mathbf{n}}_1), \ldots, (\vec{\mathbf{e}}_6.\vec{\mathbf{n}}_6))]_{6\times 6} \tag{6}$$

Using Eq. (4), the velocity of EE can be mapped to the velocity of sliders in the joint space.

3.3. Inverse dynamics of 6-PUS robot

The dynamic formulation of the 6-PUS robot is needed in section 5 for a fair evaluation of the results in comparison with FUM Stewart M450. This comparison is performed by obtaining the required forces for the robot sliders along specific paths in the Cartesian space. Fig. 6 shows the free body diagrams of the moving components of the 6-PUS robot. The free body diagram for the i^{th} leg includes reaction forces and body weights. Reaction force of the spherical joint is divided into axial component, $\vec{\mathbf{F}}_{S_i}^a$, and normal component, $\vec{\mathbf{F}}_{S_i}^n$. The reaction forces and moments from the robot base are shown by $\vec{\mathbf{F}}_{b_i}$ and $\vec{\mathbf{M}}_{b_i}$, respectively. For each leg, the unit vector $\vec{\boldsymbol{e}}_{\boldsymbol{i}}$ indicates positive direction of the local coordinate system along the robot rail. The point P in the moving platform's free body diagram indicates the center of mass for the moving platform with payload. The mass of each link, slider and moving platform with the payload are shown by m_l, m_s and M_T, respectively.

According to the free body diagram shown in Fig. 6a, by implementation of the Newton equation for the rigid link with slider, the forces of the spherical joints will be obtained in terms of actuators' force. Considering Fig. 6b, using the Newton-Euler equation for the moving platform about the origin of the moving coordinate, the closed-form dynamic equations of the 6-PUS manipulator in Cartesian space can be expressed as follows:

$$\mathbf{M}_{\boldsymbol{X}}\ddot{\mathbf{X}} + \mathbf{V}_{\boldsymbol{X}}\left(\mathbf{X}, \dot{\mathbf{X}}\right) + \mathbf{G}_{\boldsymbol{X}} = \mathbf{J}^T\vec{\mathbf{F}}^{ac} + \begin{bmatrix} \vec{\mathbf{F}}_{ext} \\ \vec{\mathbf{r}}_P \times \vec{\mathbf{F}}_{ext} + \vec{\mathbf{M}}_{ext} \end{bmatrix} \tag{7}$$

where, $\mathbf{X}$ is the generalized coordinate vector in Cartesian space and $\vec{\mathbf{F}}^{ac}$ is the matrix containing the driving forces of the sliders, $\vec{\mathbf{F}}_{p_i}$. Interested readers are referred to [22] for further details.

4. Optimum design criteria

The most important issue in implementing an optimization algorithm is to define the objective function. In this case, it is accompanied by the optimization indices, to improve the performance of a robot. Indices for robots performance assessment

Please cite this article as: S.N. Nabavi, M. Shariatee and J. Enferadi et al., Parametric design and multi-objective optimization of a general 6-PUS parallel manipulator, Mechanism and Machine Theory, https://doi.org/10.1016/j.mechmachtheory.2020.103913

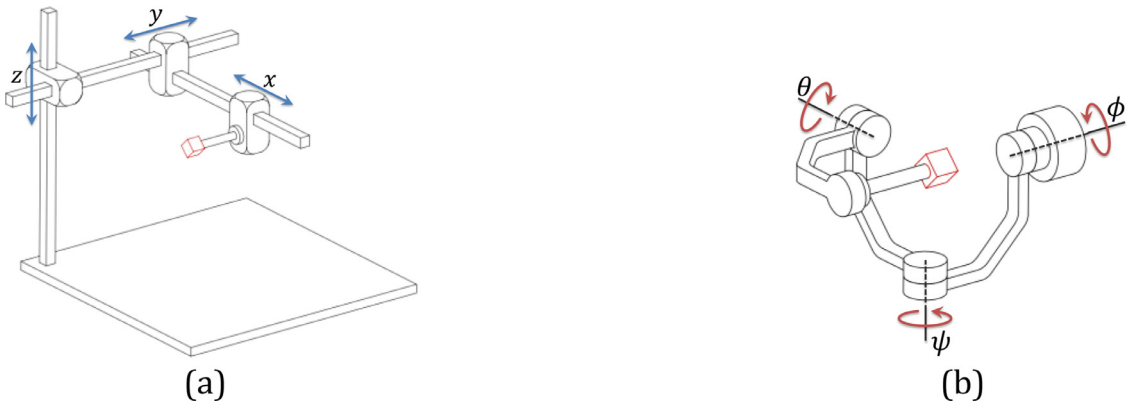

Fig. 7. a) Gantry robot, b) Gimbal robot

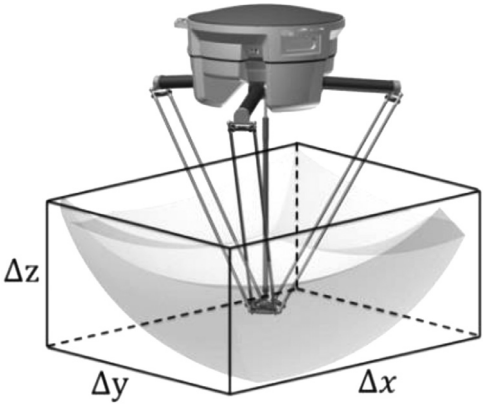

Fig. 8. The circumscribed cube of the Delta robot workspace

are divided into two categories, i.e. kinematic and dynamic indices. To design parallel robots, different indices have been defined by researchers . Each index has its own advantages and disadvantages. In the following, three indices are presented, in order to optimize the 6-PUS parallel robot.

4.1. Workspace performance index

The amount of robot workspace may be large or small. However, it is important to consider workspace with respect to the robot footprint and link length to have a fair evaluation of robot workspace [13]. This is explained by the two following examples. First, consider a gantry robot as shown in Fig. 7a. The gantry robot is able to cover a virtual cubic volume defined in Cartesian space. This is the result of their structural feature in which actuators can independently obtain any possible value within their range. The same fact is true for the gimbal structures as depicted in Fig. 7b. Unlike the gantry robot, spherical coordinates are used to show the workspace volume for a gimbal robot. These two robots represent two examples of spatial robots having the most efficient workspace with single actuation scheme, i.e. translational or rotational.

For instance, Fig. 8 shows the workspace of a translational parallel robot best known as Delta manipulator. The circumscribed cube of this workspace is the equivalent workspace of a Cartesian robot. Clearly, the higher the ratio of the robot workspace to that of this cube, the better.

Therefore, its translational workspace index, W_T, is proposed as follows,

$$W_T = \frac{\int dw_T}{\Delta x \Delta y \Delta z} = \frac{\int\int\int dxdydz}{\Delta x \Delta y \Delta z} \tag{8}$$

where dw_T is the infinitesimal volume of the translational workspace and Δx, Δy and Δz are the length of the circumscribed cube sides of translational workspace. W_T is a normalized index between zero and one. As this index approaches one, the robot design attains its optimal condition from workspace efficiency aspect. Similarly, the rotational workspace index, W_R, can be proposed.

$$W_R = \frac{\int dw_R}{\Delta\phi \Delta\theta \Delta\psi} = \frac{\int\int\int d\phi d\theta d\psi}{\Delta\phi \Delta\theta \Delta\psi} \tag{9}$$

Please cite this article as: S.N. Nabavi, M. Shariatee and J. Enferadi et al., Parametric design and multi-objective optimization of a general 6-PUS parallel manipulator, Mechanism and Machine Theory, https://doi.org/10.1016/j.mechmachtheory.2020.103913

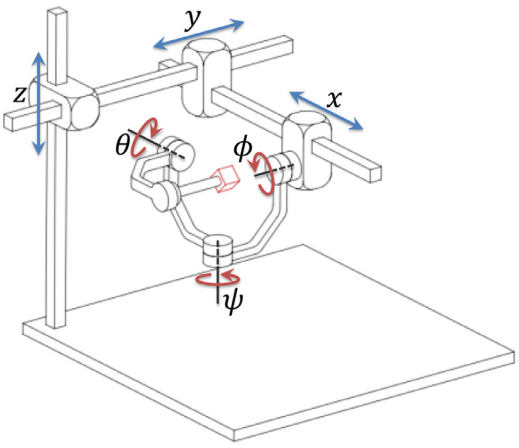

Fig. 9. A general robot with combined rotational and translational motion

where, dw_R is the infinitesimal volume of rotational workspace and $\Delta\phi$, $\Delta\theta$ and $\Delta\psi$ are the length of the circumscribed cube sides of the rotational workspace. The W_R index is also normalized and takes on values between zero and one.

Now, suppose a gimbal robot connected to a gantry robot instead of its end-effector. In this case, it is expected that the robot could easily cover any arbitrary combination of translational and rotational movements.

The presented robot in Fig. 9 could be used as a good benchmark for evaluating workspace performance of robots with combined motions. Therefore, general workspace index, W_G, is proposed as shown in Eq. (10).

$$W_G = \frac{\int \dots \int dxdydzd\phi d\theta d\psi}{\Delta x \Delta y \Delta z \Delta\phi \Delta\theta \Delta\psi} \tag{10}$$

In this paper, the goal is to evaluate workspace efficiency of 6-DoF parallel robots. It should be noted that due to limited workspace, motion cueing algorithm tries to produce the acceleration as close as to the real vehicle to give the driver a realistic sense of motion. To get ready for next motion, simulator returns to home under sensory threshold of human brain. This procedure is known as washout mechanism [28]. Thus, in order to integrate general workspace index for motion simulation applications, Eq. (10) is modified as follows:

$$W_{G,H} = W_{T,H} W_{R,H} \tag{11}$$

In this new index, $W_{T,H}$ represents the translational workspace index for fixed rotational DoF in home position, i.e. $\phi = \theta = \psi = 0$, and $W_{R,H}$ represents the rotational workspace index for fixed translational DoF in home position, i.e. $x = y = 0,\ z = Z_h$. As a result of this simplification, computational efficiency is significantly improved.

4.2. Dexterity index

The dexterity of a robot is obtained by analyzing the Jacobian matrix which depends on robot position [29,30]. The Jacobian matrix maps the velocity vector of the actuated joints, $\dot{\mathbf{q}}$, to the velocity vector of the end-effector, $\mathbf{t}_{EE}$. The considered joint velocity as $\dot{\mathbf{q}} \cdot \dot{\mathbf{q}} = 1$, represents a hyper-sphere. The Jacobian matrix maps it to a hyper-ellipsoid in Cartesian space. The radii of the mapped ellipse are the geometrical illustration for singular values of the Jacobian matrix. By gradual change of the robot's manipulability ellipses to a sphere, the robot's maneuverability will increase. In fact, reshaping and reorienting manipulability ellipses can be considered as a measure of how maneuverable a robot is.

The dexterity index of a robot, DI, is determined by the concept of inverse condition number of the Jacobian matrix, ranging between zero and one. The value of zero and one indicate the singularity conditions and the isotropic conditions for the robot, respectively. In order to represent global dexterity of a robot in the entire workspace by a single number, Eq. (12) is used.

$$\mathrm{GDI} = \frac{\int_w \mathrm{DI}\ dw}{\int_w dw} \tag{12}$$

where dw is the volume element of the workspace. A robot is fully isotropic, if the value of GDI, global dexterity index, is equal to one.

When a robot has only translational or rotational degrees of freedom, the use of kinematic indices defined for performance evaluation will result in a trustworthy assessment. Sometimes, designers face problems using kinematics indices. When a robot undergoes translational and rotational motions simultaneously, because of the non-homogeneity of the Jacobian matrix, kinematic performance indices are not applicable and it may not give a proper interpretation and a reliable result. To overcome this problem, researchers have proposed various methods to homogenize the arrays of Jacobin matrix

Please cite this article as: S.N. Nabavi, M. Shariatee and J. Enferadi et al., Parametric design and multi-objective optimization of a general 6-PUS parallel manipulator, Mechanism and Machine Theory, https://doi.org/10.1016/j.mechmachtheory.2020.103913

[31–33]. A parameter called the characteristic length could be used to homogenize the robot's Jacobian matrix instead of changing the kinematic model [12]. The homogeneous Jacobian matrix is constructed as follows:

$$\mathbf{J}_h \equiv \mathbf{J}\ \mathrm{diag}\left(\frac{1}{L},\ \frac{1}{L}, \frac{1}{L}, 1, 1, 1\right) \tag{13}$$

where the parameter L is an arbitrary constant used to make Jacobian arrays dimensionless. In this paper, the parameter Z_h is used as the characteristic length.

4.3. Kinetic energy index

In the discussion of non-homogeneity of the Jacobian matrix for robots having combined degrees of freedom, some researchers have proposed other indices using the concepts of power and kinetic energy [1,34], which have the same unit in translational and rotational movements. A power-based homogeneous performance index constitutes a physically consistent system, regardless of the joint types or degrees of freedom.

Similar to the concept of power, the kinetic energy quantity can also be a suitable tool for defining performance indices. Recently a new payload specific performance index has also been proposed which makes use of the concept of transferred kinetic energy from actuators to the payload of a robot. For this purpose, one should consider the kinetic energy of a manipulator payload as follows:

$$\mathcal{K}_P = \frac{1}{2} M_P {}^{\mathcal{P}}\vec{\mathrm{V}}_P \cdot {}^{\mathcal{P}}\vec{\mathrm{V}}_P + \frac{1}{2} {}^{\mathcal{P}}\vec{\Omega}_P^{\mathrm{T}\,\mathcal{P}}\mathrm{I}_P\, {}^{\mathcal{P}}\vec{\Omega}_P \tag{14}$$

where, M_P and ${}^{\mathcal{P}}\mathbf{I}_P$ are the mass of payload and the inertia tensor of payload, respectively. The leading superscript $\mathcal{P}$ indicates that the defining parameter is expressed in coordinate system $\{\mathcal{P}\}$ located at the center of the robot payload. ${}^{\mathcal{P}}\vec{\mathbf{V}}_{\boldsymbol{P}}$ and ${}^{\mathcal{P}}\vec{\boldsymbol{\Omega}}_{\boldsymbol{P}}$ are the translational and rotational velocity vectors of the payload that relate to the actuated joint velocities, ${}^{\mathcal{P}}\dot{\vec{\mathbf{q}}}$, as follows:

$${}^{\mathcal{P}}\dot{\vec{\mathbf{q}}} = {}^{\mathcal{P}}\mathbf{J}\ {}^{\mathcal{P}}\dot{\vec{\mathcal{X}}}_P \tag{15}$$

where, ${}^{\mathcal{P}}\dot{\vec{\mathcal{X}}}_{\boldsymbol{P}} = [{}^{\mathcal{P}}\vec{\mathbf{V}}_{\boldsymbol{P}}^{\boldsymbol{T}} \quad {}^{\mathcal{P}}\vec{\boldsymbol{\Omega}}_P^T]^T$ is the twist vector of the payload and ${}^{\mathcal{P}}\mathbf{J}$ is the Jacobian matrix. This matrix can be partitioned into translational and rotational segments as ${}^{\mathcal{P}}_{\boldsymbol{T}}\mathbf{J}$ and ${}^{\mathcal{P}}_{\boldsymbol{R}}\mathbf{J}$, respectively. By defining these parameters and substituting Eq. (15) into Eq. (14), the kinetic energy of the payload in terms of actuated joint velocities can be expressed as Eq. (16).

$$\mathcal{K}_P = {}^{\mathcal{P}}\dot{\vec{\mathbf{q}}}^T \left(\frac{1}{2} M_P T^{\mathcal{P}}\mathbf{J}^{-\boldsymbol{T}} T^{\mathcal{P}}\mathbf{J}^{-1} + \frac{1}{2} R^{\mathcal{P}}\mathbf{J}^{-\mathbf{T}\,\mathcal{P}}\mathbf{I}_P R^{\mathcal{P}}\mathbf{J}^{-1}\right) {}^{\mathcal{P}}\dot{\vec{\mathbf{q}}} = {}^{\mathcal{P}}\dot{\vec{\mathbf{q}}}^T \mathcal{K}^{\mathcal{P}}\dot{\vec{\mathbf{q}}} \tag{16}$$

Defining the kinetic energy index, KEI, as Eq. (17), one can obtain information about the possibility of kinetic energy transfer to the payload.

$$\mathrm{KEI} = \frac{1}{\sqrt{\Lambda^*_{\max}/\Lambda^*_{\min}}} \tag{17}$$

where $\Lambda^*_{\max}$ and $\Lambda^*_{\min}$ are the maximum and minimum eigenvalues of the matrix $\mathcal{K}$ respectively. According to the reference [1], it can be easily proved that these eigenvalues represent the maximum and minimum kinetic energy saved by the payload of the robot respectively. Depending on the robot configuration, KEI varies in an interval from zero to one in the entire workspace. While this index stands for a local representation of robot energy transfer possibility, the global kinetic energy index, GKEI, is equal to:

$$\mathrm{GKEI} = \frac{\int_{\mathrm{w}} \mathrm{KEI}\ dw}{\int_{\mathrm{w}} dw} \tag{18}$$

where, dw is the volume element of the workspace. As the value of KEI approaches one, it can be ensured that a uniform kinetic energy is transferred to the payload of the robot for all feasible joint velocities. The zero value for KEI indicates that for the specific combination of feasible joint velocities, the kinetic energy is not transferable to the payload by actuators, and such robot is not acceptable from the design point of view. Since this index does not depend on the units used in defining motion, it can undoubtedly be used in the design of the 6-PUS parallel manipulator.

5. Multi-objective optimization of the 6-PUS robot

In robot synthesis similar to usual daily issues, several criteria are involved at the same time in designers' decision making. Multi-objective optimization is a systematic thinking method which converts ordinary decision making process to a mathematical problem. Classical methods break a single multi-objective problem down into multiple single-objective problems, although evolutionary methods consider the problem as a whole and try to fulfill the objectives simultaneously. Evolutionary multi-objective optimization overcomes common classical challenges such as appropriate weighting. For the problem of finding 6-PUS architecture alternatives, genetic algorithm is used as an evolutionary technique which proposes a set of variant trade-off solutions better known as Pareto front. The multi-objective optimization goal is as follows:

$$\begin{aligned} &\text{Minimize } F_i(x_1, x_2, \ldots, x_n);\ \text{for } i = 1:m \\ &\text{Subject to}:\ G_i(x_1, x_2, \ldots, x_n) = 0,\ H_k(x_1, x_2, \ldots, x_n) \le 0;\ \text{for } j = 1:p,\ k = 1:q \end{aligned} \tag{19}$$

Please cite this article as: S.N. Nabavi, M. Shariatee and J. Enferadi et al., Parametric design and multi-objective optimization of a general 6-PUS parallel manipulator, Mechanism and Machine Theory, https://doi.org/10.1016/j.mechmachtheory.2020.103913

Table 3
The range of optimization variables for the 6-PUS robot.

Variable	d_b	d_p	p_0	β	γ
Unit	(m)	(m)	(m)	(°)	(°)
Range	$0.10 < d_b < 0.25$	$0.12 < d_p < 0.25$	$0.2 < p_0 < 0.4$	$0 < \beta < 90$	$20 < \gamma < 50$

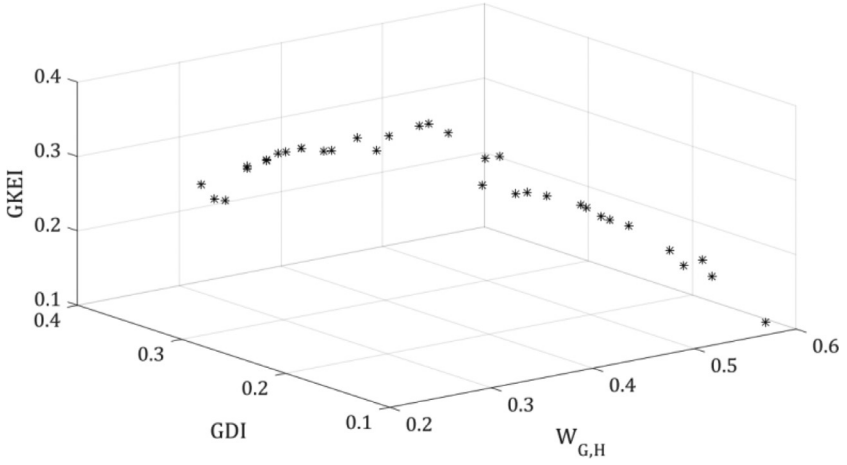

Fig. 10. Pareto optimal set based on workspace, dexterity and kinetic energy indices

where, F_i is the objective functions, G_i and H_k are the linear and nonlinear constraint functions, respectively, and x_i are the design parameters [35].

In order to find a set of solutions for the multi-objective problem of the 6-PUS parallel robot performance optimization, three indices of workspace, dexterity and kinetic energy are utilized. In order to check out whether a randomly chosen robot could be nominated as optimum solution, the first step is that it must fulfill the necessary condition of meeting the desired workspace constraints just as those of the laboratory FUM Stewart M450.

$$\mathrm{W}_{G,H} = \mathrm{W}_{T,H}\mathrm{W}_{R,H} \rightarrow \max \tag{20}$$

$$\mathrm{GDI} = \frac{\int \ldots \int \mathrm{DI}\ dw_T dw_R}{\int \ldots \int dw_T dw_R} \rightarrow \max \tag{21}$$

$$\mathrm{GKEI} = \frac{\int \ldots \int \mathrm{KEI}\ \mathrm{dw_T dw_R}}{\int \ldots \int \mathrm{dw_T dw_R}} \rightarrow \max \tag{22}$$

where $dw_T = dxdydz$ and $dw_R = d\phi d\theta d\psi$ are the elements of the translational and rotational workspace, respectively. The three parameters r_b, r_p and Z_h are considered constant through the whole optimization. These constant values are integrated from FUM Stewart M450 design parameters. As a result, the volume occupied by the two robots, 6-UPS and 6-PUS, is the same. The constant parameters are equal to $r_b = 0.700$ m, $r_p = 0.462$ m and $Z_h = 1.170$ m. In addition, five parameters are considered as the optimization algorithms variables for the 6-PUS robot as stated before. Two parameters d_b and d_p are for base and moving platform, two parameters β and γ are for the angle of the robot motion rails, and the parameter p_0 is for the initial position of the sliders. Dynamic parameters as well as the stroke length of actuators are considered to be the same as the values of the FUM Stewart M450 robot. Table 3 gives information on the range of variables.

Fig. 10 shows the Pareto front solutions for the 6-PUS robot. As the figure shows, each of the presented points is an optimal robot having different portions from each index.

The mutual interaction of each pair of indices for the 6-PUS robot is shown in Fig. 11. As $\mathrm{W}_{G,H}$ increases, GDI slightly decreases. In contrast, for greater GDIs, GKEI linearly increases. Although a continuous trend could not be considered for mutual investigation of $\mathrm{W}_{G,H}$ and GKEI, by increasing $\mathrm{W}_{G,H}$ from 0.45 to 0.6, GKEI dramatically decreases. However, these results are highly affected by the imposed constraints. Therefore, for a desired workspace, a general unconstrained optimization would obtain more desirable results.

A designer can choose a robot according to the prior index with respect to the desired application. For comparison with respect to the FUM Stewart M450, specifications of three optimal 6-PUS robots each acting as a candidate of performance indices from the Pareto front as highlighted on Fig. 11, are shown in Table 4.

It is worth mentioning that all optimal robots cover the desired workspace. The actual workspace of these robots are compared with the desired and actual workspace of the FUM Stewart robot in Table 5. The positive point about optimum

Please cite this article as: S.N. Nabavi, M. Shariatee and J. Enferadi et al., Parametric design and multi-objective optimization of a general 6-PUS parallel manipulator, Mechanism and Machine Theory, https://doi.org/10.1016/j.mechmachtheory.2020.103913

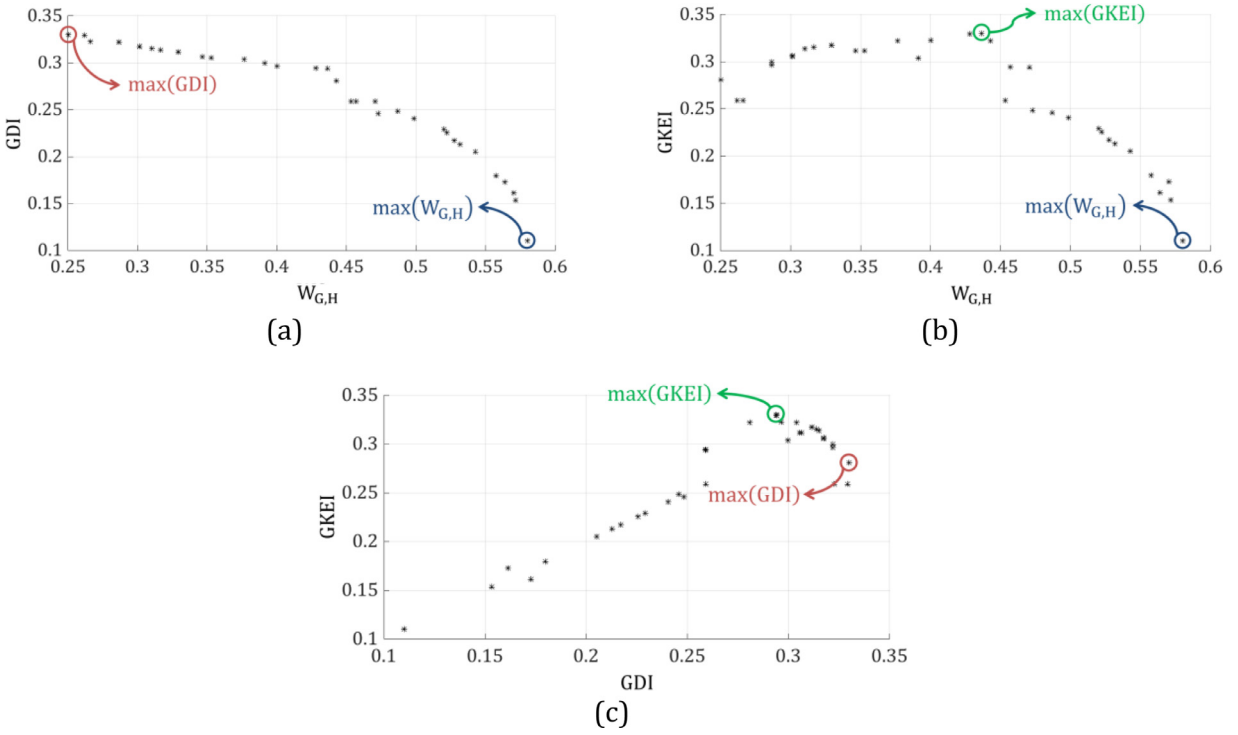

Fig. 11. The interaction between indices, a) GDI- $W_{G,H}$ Pareto optimal set, b) GKEI- $W_{G,H}$ Pareto optimal set, c) GKEI- GDI Pareto optimal set

Table 4
The characteristics of optimized 6-PUS robots based on workspace, dexterity, kinetic energy.

Optimized robot			Optimized parameters					Configuration of the robot
			d_b(cm)	d_p(cm)	p_0(cm)	β (°)	γ (°)	
I	$\mathbf{W_{G,H}}$ GDI GKEI	0.11 0.10 0.12	18.0	23.8	30.1	13	42	
II	$\mathbf{W_{G,H}}$ GDI GKEI	0.08 0.34 0.30	10.3	12.6	32.8	28	42	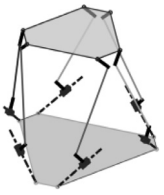
III	$\mathbf{W_{G,H}}$ GDI GKEI	0.05 0.26 0.35	10.0	10.3	28.9	18	50	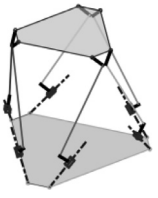

I- Optimized robot based on the maximum $\mathbf{W_{G,H}}$ from Pareto front.
II- Optimized robot based on the maximum **DI** from Pareto front.
III- Optimized robot based on the maximum **KEI** from Pareto front.

Please cite this article as: S.N. Nabavi, M. Shariatee and J. Enferadi et al., Parametric design and multi-objective optimization of a general 6-PUS parallel manipulator, Mechanism and Machine Theory, https://doi.org/10.1016/j.mechmachtheory.2020.103913

Table 5
Comparing workspaces of three optimal 6-PUS robot architectures with the FUM Stewart M450.

Robot	DoF	Translational Movement						Rotational Movement					
		Surge (cm)		Sway (cm)		Heave (cm)		Roll (°)		Pitch (°)		Yaw (°)	
	Desired Workspace	± 25		± 25		± 12		± 14		± 14		± 20	
FUM Stewart M450	Actual	−38	+38	−41	+41	−13	+21	−25	+17	−19	+19	−48	+48
6-PUS (I)	Workspace	−37	+37	−36	+41	−12	+14	−16	+14	−15	+15	−42	+42
6-PUS (II)		−26	+26	−26	+30	−17	+14	−16	+20	−18	+18	−29	+29
6-PUS (III)		−30	+30	−33	+33	−14	+20	−23	+16	−17	+17	−37	+37

I- Optimized robot based on the maximum $\mathbf{W}_{G,H}$ from Pareto front.
II- Optimized robot based on the maximum **DI** from Pareto front.
III- Optimized robot based on the maximum **KEI** from Pareto front.

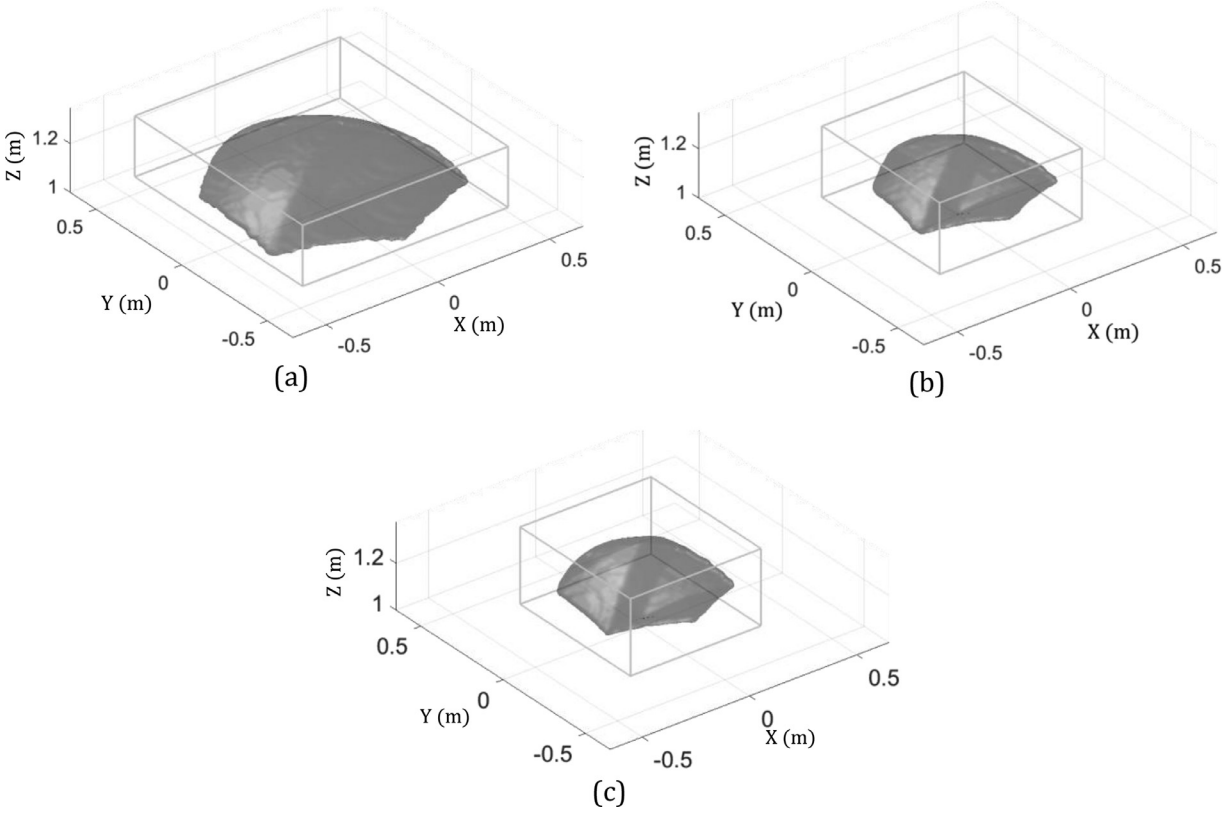

Fig. 12. Translational workspace for $\phi = \theta = \psi = 0$ with circumscribed cube for the 6-PUS robot, a) Type-I, b) Type-II and c) Type-III

6-PUS robots listed in the table is that they all have an actual workspace smaller than that of the FUM Stewart M450 robot. In fact, the closer the actual workspace of a robot is to the desired workspace, the less actuator force is required to navigate the robot. Also, the following force analysis section verifies the robot with smaller workspace is more efficient in terms of actuator force.

In Figs. 12 and 13 translational workspace for fixed rotational DoF in home position, i.e. $\phi = \theta = \psi = 0$, and rotational workspace index for fixed translational DoF in home position, i.e. $x = y = 0,\ z = Z_h$, with the circumscribed cube for the three types of 6-PUS robot are shown respectively.

Despite the fact that a design may seem to be an optimum one with respect to performance indices theoretically, the implementation of such system might not be possible in practice. Too much actuator forces could be mentioned as one of the most common example of such limits. Hence, to select a suitable alternative for the FUM Stewart M450 robot from the three optimum 6-PUS architectures, the sufficient condition is to have lower forces in comparison to the Stewart. Therefore, static and dynamic actuator forces are provided in Table 6 for comparison. In order to compare dynamic forces, six trajectories for each degree of freedom are defined within the desired workspace. Trajectories in each direction are generated in such a way that the robot reaches its maximum allowed velocity and acceleration along the path [36]. The allowed velocity and acceleration for translational motions are 0.5 m/s and 9.81 m/s^2, as well as 50°/s and 500°/s^2 for rotational mo-

Please cite this article as: S.N. Nabavi, M. Shariatee and J. Enferadi et al., Parametric design and multi-objective optimization of a general 6-PUS parallel manipulator, Mechanism and Machine Theory, https://doi.org/10.1016/j.mechmachtheory.2020.103913

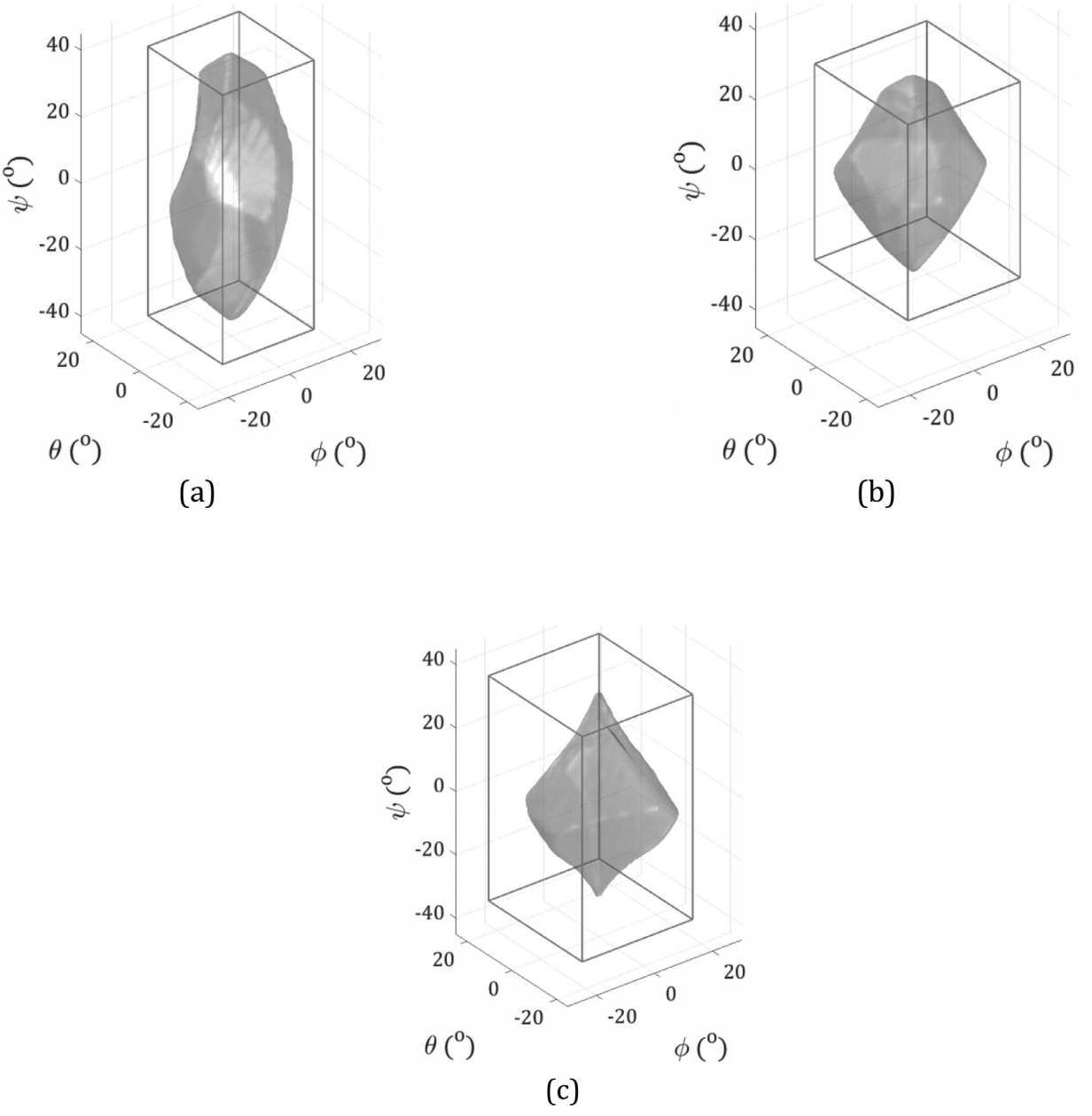

Fig. 13. Rotational workspace for $x = y = 0,\ z = Z_h$ with circumscribed cube for the 6-PUS robot, a) Type-I, b) Type-II and c) Type-III

tions. The maximum dynamic force is calculated among six robot actuators in all six trajectories. Likewise, the maximum static force is calculated in different translational and rotational configurations in the entire actual workspace of the 6-PUS robot.

Among the four robots presented for comparison, Type-I robot undergoes the most severe static or dynamic forces as shown in Table 6. Definitely, this is the result of excessive focus on maximizing workspace index. In contrast, Type-II and Type-III robots have successfully reduced actuator forces compared to the FUM Stewart M450. Designers should take into consideration that static force plays a dominant role in determination of robot actuators and their cost consequently. This is because actuator's power consumption in stationary positions is continuous, whereas it instantaneously increases during robot motion simulation. Industrial servo motors are usually able to deliver three times more torque than their rated torque for instantaneous dynamic situations. Considering all these facts, Type-II robot is a better alternative for the Stewart counterpart.

Please cite this article as: S.N. Nabavi, M. Shariatee and J. Enferadi et al., Parametric design and multi-objective optimization of a general 6-PUS parallel manipulator, Mechanism and Machine Theory, https://doi.org/10.1016/j.mechmachtheory.2020.103913

Table 6
Comparing maximum static and dynamic force of three optimal 6-PUS robot architectures with FUM Stewart M450.

Robot	FUM Stewart M450	6-PUS (I)	6-PUS (II)	6-PUS (III)
Maximum dynamic force	6.9 KN	7.7 KN	5.5 KN	5.8 KN
Maximum static force	4.7 KN	24 KN	2.4 KN	3.1 KN
Configuration of the robot in maximum static force	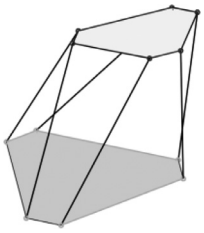	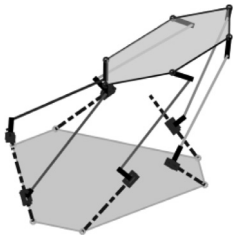	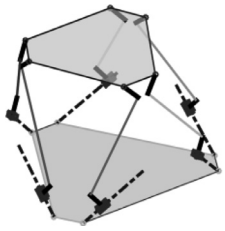	

I- Optimized robot based on the maximum $\mathbf{W}_{G,H}$ from Pareto front.
II- Optimized robot based on the maximum **DI** from Pareto front.
III- Optimized robot based on the maximum **KEI** from Pareto front.

6. Conclusion

The 6-UPS Stewart robot is the most commonly used structure for today's motion simulators and has been the focus of many studies. These robots use rather complicated linear jacks that results in a complicated mechanical design. Therefore, the question is whether we can find a different parallel robot structure that offers similar motion characteristics while increasing performance and lowering mechanical structural cost or not.

In this paper, a general 6-PUS parallel robot is considered and compared with the 6-UPS Stewart robot. The 6-PUS parallel robot potentially lowers the actuators center of mass and significantly reduces power consumption in stationary positions, i.e. maximum static force. Furthermore, in contrast with the Stewart robot, six actuators are placed on the fixed base resulting in lowering structural system cost. To do this, the FUM Stewart M450 is considered as a comparison baseline. A new modified workspace index $W_{G,H}$ specifically designed for motion simulators is introduced. This index takes advantage of return to home position for each subsequent motion used by the motion simulators. Additionally, the proposed index simultaneously considers combined translational and rotational degrees of freedom in one index. The simplified formulation of the proposed index can serve as a criterion for workspace efficiency evaluation of motion simulators. Two additional performance indices, i.e. GDI and GKEI is used and a multi-objective optimization of a general 6-PUS robot is presented. The GDI index helps to reduce actuator forces whereas it maintains the robot workspace far from singular positions. The recently introduced GKEI index, defined based on transferred kinetic energy to the payload is also used. This index overcomes the problem of non-homogeneity of the Jacobian matrix in the same way as the GDI index does. As a result of multi-objective optimization, a Pareto optimal set was provided. Designers can choose a solution from this graph to synthesize a robot with respect to the application. The Pareto front is limited to finding appropriate 6-PUS alternatives for the FUM Stewart M450 considering the same footprint and desired workspace as constraints. Among the Pareto solutions, three robots were chosen for comparison. Each of these robots represents maximum $W_{G,H}$, GDI and GKEI indices, respectively.

The results indicate that the process successfully identified a 6-PUS robot that meets the required workspace while reducing the actuator's static and dynamic forces by 49% and 20%, respectively. The contributions of this study are:

1 Presentation of a new workspace index designed for motion simulators that simultaneously considers both translational and rotational degrees of freedom,
2 Overcoming dimensional non-homogeneity problem for manipulators with combined motions,
3 Presentation of a general method that allows comparing various robot structures and architectures with common dimensional constraints,
4 Successful identification of an optimum 6-PUS robot that significantly decreases static and dynamic forces in comparison to the equivalent Stewart. This paves the way for lower cost parallel robot simulators.

Declaration of Competing Interest

The authors declare that they have no known competing financial interests or personal relationships that could have appeared to influence the work reported in this paper.

References

[1] S.N. Nabavi, A. Akbarzadeh, J. Enferadi, I. Kardan, A homogeneous payload specific performance index for robot manipulators based on the kinetic energy, Mech. Mach. Theory 130 (2018) 330–345.

Please cite this article as: S.N. Nabavi, M. Shariatee and J. Enferadi et al., Parametric design and multi-objective optimization of a general 6-PUS parallel manipulator, Mechanism and Machine Theory, https://doi.org/10.1016/j.mechmachtheory.2020.103913

[2] Y. Chen, F. Dong, Robot machining: recent development and future research issues, Int. J. Adv. Manuf. Technol. 66 (2013) 1489–1497.
[3] M. Shariatee, A. Akbarzadeh Tootoonchi, S.A. Mousavi Mohammadi, S. Alimardani, Design of an economical SCARA robot for industrial applications, in: 2nd ICRoM International Conference on Robotics and Mechatronics, 2014.
[4] J. Freeman, G. Watson, Y. Papelis, T. Lin, A. Tayyab, R. Romano, et al., "The Iowa driving simulator: an implementation and application overview," SAE Technical Paper 0148-7191, 1995.
[5] V. Gough, Universal tyre test machine, in: Proceedings of the FISITA 9th International Technical Congress, 1962, London, 1962, pp. 117–137.
[6] H. Kalani, A. Akbarzadeh, S.N. Nabavi, S. Moghimi, Dynamic modeling and CPG-based trajectory generation for a masticatory rehab robot, Intel. Serv. Robot. 11 (2018) 187–205.
[7] M. Weck, D. Staimer, Parallel kinematic machine tools–current state and future potentials, CIRP Ann. Manuf. Technol. 51 (2002) 671–683.
[8] A. Martini, Gravity compensation of a 6-UPS parallel kinematics machine tool through elastically balanced constant-force generators, FME Trans. 46 (2018) 10–16.
[9] M. Zoppi, D. Zlatanov, R. Molfino, Kinematics analysis of the Exechon tripod, in: ASME 2010 International Design Engineering Technical Conferences and Computers and Information In Engineering Conference, 2010, pp. 1381–1388.
[10] G.F. Bär, G. Weiß, Kinematic analysis of a pentapod robot, J. Geom. Gr 10 (2006) 173–182.
[11] M.J. Lum, J. Rosen, M.N. Sinanan, B. Hannaford, Optimization of a spherical mechanism for a minimally invasive surgical robot: theoretical and experimental approaches, IEEE Trans. Biomed. Eng. 53 (2006) 1440–1445.
[12] O. Ma, J. Angeles, Optimum architecture design of platform manipulators, in: Advanced Robotics, 1991.'Robots in Unstructured Environments', 91 ICAR., Fifth International Conference on, 1991, pp. 1130–1135.
[13] J. Enferadi, R. Nikrooz, The performance indices optimization of a symmetrical fully spherical parallel mechanism for dimensional synthesis, J. Intel. Robot. Syst. (2018) 1–17.
[14] K. Gupta, On the nature of robot workspace, Int. J. Robot. Res. 5 (1986) 112–121.
[15] T. Yoshikawa, Analysis and control of robot manipulators with redundancy, in: Robotics Research: The First International Symposium, 1984, pp. 735–747.
[16] J.K. Salisbury, J.J. Craig, Articulated hands: force control and kinematic issues, Int. J. Robot. Res. 1 (1982) 4–17.
[17] C.M. Gosselin, The optimum design of robotic manipulators using dexterity indices, Rob. Autom. Syst. 9 (1992) 213–226.
[18] C. Gosselin, Stiffness mapping for parallel manipulators, IEEE Trans. Robot. Autom. 6 (1990) 377–382.
[19] J.-P. Merlet, C. Gosselin, Nouvelle architecture pour un manipulateur parallèle à six degrés de liberté, Mech. Mach. Theory 26 (1991) 77–90.
[20] I.A. Bonev, J. Ryu, A geometrical method for computing the constant-orientation workspace of 6-PRRS parallel manipulators, Mech. Mach. Theory 36 (2001) 1–13.
[21] M. Honegger, A. Codourey, E. Burdet, Adaptive control of the hexaglide, a 6 dof parallel manipulator, in: Robotics and Automation, 1997. Proceedings., 1997 IEEE International Conference on, 1997, pp. 543–548.
[22] S.N. Nabavi, A. Akbarzadeh, J. Enferadi, Closed-form dynamic formulation of a general 6-P US robot, J. Intel. Robot. Syst. (2019) 1–14.
[23] S.N. Nabavi, A. Akbarzadeh, J. Enferadi, A study on kinematics and workspace determination of a general 6-P US robot, J. Intel. Robot. Syst. 91 (2018) 351–362.
[24] M. Toz, S. Kucuk, Dexterous workspace optimization of an asymmetric six-degree of freedom Stewart–Gough platform type manipulator, Rob. Autom. Syst. 61 (2013) 1516–1528.
[25] S. Khan, K. Andersson, J. Wikander, Jacobian matrix normalization-a comparison of different approaches in the context of multi-objective optimization of 6-DOF haptic devices, J. Intel. Robot. Syst. 79 (2015) 87–100.
[26] J. Angeles and J. Angeles, Fundamentals of Robotic Mechanical Systems vol. 2: Springer, 2002.
[27] I. Fassi, G. Legnani, D. Tosi, Geometrical conditions for the design of partial or full isotropic hexapods, J. Robot. Syst. 22 (2005) 507–518.
[28] D. Cleij, J. Venrooij, P. Pretto, M. Katliar, H. Bülthoff, D. Steffen, et al., Comparison between filter-and optimization-based motion cueing algorithms for driving simulation, Transp. Res. Part F: Traffic Psychol. Behav. (2017).
[29] J.-P. Merlet, Parallel Robots, 128, Springer Science & Business Media, 2006.
[30] R. Kelaiaia, O. Company, A. Zaatri, Multiobjective optimization of a linear Delta parallel robot, Mech. Mach. Theory 50 (2012) 159–178.
[31] J. Angeles, The design of isotropic manipulator architectures in the presence of redundancies, Int. J. Robot. Res. 11 (1992) 196–201.
[32] S. Patel, T. Sobh, Manipulator performance measures-a comprehensive literature survey, Journal of Intelligent & Robotic Systems 77 (2015) 547–570.
[33] M. Hosseini, H. Daniali, Weighted local conditioning index of a positioning and orienting parallel manipulator, Scientia Iranica 18 (2011) 115–120.
[34] I. Mansouri, M. Ouali, The power manipulability–A new homogeneous performance index of robot manipulators, Rob. Comput. Integr. Manuf. 27 (2011) 434–449.
[35] E. Zitzler, Evolutionary algorithms for multiobjective optimization: Methods and applications, 63, Citeseer, 1999.
[36] M. Shariatee, A. Akbarzadeh, N. Nabavi, Design of a Pneumatic Weight Compensation System for the FUM Stewart Robot, in: 2017 5th RSI International Conference on Robotics and Mechatronics (ICRoM), 2017, pp. 624–629.

Please cite this article as: S.N. Nabavi, M. Shariatee and J. Enferadi et al., Parametric design and multi-objective optimization of a general 6-PUS parallel manipulator, Mechanism and Machine Theory, https://doi.org/10.1016/j.mechmachtheory.2020.103913